Low-temperature phase transformation from nanotube to sp^3 superhard carbon phase*

Xu Ning(徐 宁)[a)†], Li Jian-Fu(李建福)[b)], Huang Bo-Long(黄勃龙)[b)], and Wang Bao-Lin (王保林)[a)‡]

[a)] *Department of Physics, Yancheng Institute of Technology, Yancheng* 224051, *China*
[b)] *Department of Physics and Materials Science, City University of Hong Kong, Hong Kong SAR*

(Received 11 November 2014; revised manuscript received 14 January 2015; published online 10 April 2015)

Numerous new carbon allotropes have been uncovered by compressing carbon nanotubes based on our computational investigation. The volume compression calculations suggest that these new phases have a very high anti-compressibility with a large bulk modulus (B_0). The predicted B_0 of new phases is larger than that of *c*-BN (373 GPa) and smaller than that of diamond (453 GPa). All of the predicted structures are superhard transparent materials with a larger band gap and possess the covalent characteristics with sp^3-hybridized electronic states. The simulated results will help us better understand the structural phase transition of cold-compressed carbon nanotubes.

Keywords: low-temperature phase transformation, superhard carbon phase

PACS: 61.66.Bi, 61.50.Ks, 62.50.–p, 78.30.Am **DOI:** 10.1088/1674-1056/24/6/066102

1. Introduction

Carbon exhibits numerous allotropes [graphite, carbon nanotubes (CNTs), fullerene, amorphous carbon, cubic and hexagonal diamond] because of its ability to form sp-, sp^2-, and sp^3-hybridized bonds.[1–3] As is well known, graphite can be converted into the cubic or hexagonal diamond at pressures above 15 GPa and high temperatures above 1300 K.[4–9] In contrast, cold-compressions of single-walled and multi-walled CNTs result in superhard carbon allotropes, which were found to be intrinsically different from cubic and hexagonal diamond.[10–16] The unknown carbon phase compressed at above 75 GPa can be quenched at room temperature,[10] and exhibits superior mechanical performance and higher hardness comparable to cubic diomond. In order to shed light on the puzzling structure, several hypothetical structures, such as M-carbon,[17,18] Z-carbon,[19–21] W-carbon,[22] bct-C4-carbon,[23] P-carbon and S-carbon,[24] have been proposed. Nevertheless, the crystal structure of the cold-compressed CNTs is still the subject of intense discussion in the literature up to now. In addition to the crystal structure of the cold-compressed CNTs, the collapse process itself is still not completely understood, as only indirect observation is reported. It is shown that not only the diameter,[25–29] but also the nanotube chirality or defect[30,31] determine the radial collapse pressure of CNTs.

In order to figure out the crystal structure of the cold-compressed CNTs, we present a comprehensive study of the phase transition of CNTs under compression in a preessure range from 0 to 400 GPa. Surprisingly, we find that not only cubic or hexagonal diamond, but also most of the hypothetical structures [M-carbon, Z-carbon, W-carbon, bct-C4-carbon] are obtained from the cold-compressed CNTs. In addition, numerous new carbon phases are observed. These new phases are wide-gap transparent and superhard insulators. The calculated results can help us understand the structural phase transition of cold-compressed CNTs.

2. Method

The calculations are carried out based on density functional theory within the local density approximation (LDA) as implemented in the Vienna *ab initio* simulation package (VASP).[32–34] The projector augmented wave (PAW) method is used to describe the ionic potentials.[35] A plane-wave basis with a cutoff energy of 700 eV is used to expand the wave functions of all systems considered in the present work.[36] The Brillouin zone (BZ) sample meshes for all carbon allotropes are set to be $11\times11\times11$, which are dense enough in our calculations. Forces on the ions are calculated by using the Hellmann–Feynman theorem allowing for a full geometry optimization. For simplicity and to make the simulations generic, the CNTs are orderly placed. The initial structure of the unit cell is an orthorhombic cell (cell angles: $\alpha=\beta=\gamma=90^\circ$), which possesses four ordered CNTs. Each of them stays along the axial direction (shown in Fig. 1). Four cases with different

*Project supported by the National Natural Science Foundation of China (Grant Nos. 11174242, 11204265, 11404278, 11147007, and 11274151), the Natural Science Foundation of Jiangsu Province, China (Grant No. BK2012248), and the Scientific Research Foundation of Yancheng Institute of Technology, China (Grant No. KJC2014024).

†Corresponding author. E-mail: nxu@ycit.cn
‡Corresponding author. E-mail: wangbl@ycit.edu.cn

© 2015 Chinese Physical Society and IOP Publishing Ltd

ordered CNTs are used for our initial models, which are (18, 0), (7, 0), (4, 4), and (3, 3) CNTs, respectively. Therefore, the initial cell contains one complete 64-atom (18, 0) carbon nanotube as shown in Fig. 1(a). Before our cold-compress procedure, to eliminate the van de Waals (vdW) interaction effect between the inter-walls of CNTs, we adjust the cell parameters to ensure the inter-wall distance of CNTs within each initial cell to be 5.0 Å. As to the geometry optimization, all of the cell lattice constants (a, b, and c) and angles (α, β, and γ) are set to be variable for full geometry relaxations. Regarding the topic of cold compress, we only focus on the pressure variable at zero temperature ($T = 0$ K) to illustrate the low-temperature phase transformations.

According to the above structural built-up and calculation preparations, we employ the full geometry optimization under external pressure constrain, which is called hydrostatic pressure. The whole computational investigation relating to the full cell geometry optimizations starts from 0 GPa and ends at 400 GPa in steps of 5.0 GPa.

Note that in order to evaluate the transition pressure from CNTs to the common product of high pressure, the exchange–correlation functional is described by LDA. Although LDA is a simple approximation of DFT, it can give reasonable interlayer distances and mechanical properties of CNTs due to a delicate error cancellation between exchange and correlation in comparison with the semi-local generalized gradient approximation (GGA).[37]

Another important point that should be noted is that in order to obtain the precise electronic structure of each new phase, we take the screened exchange method (sX-LDA) implemented in CASTEP code to calculate the electronic structures of the new structural models with sX-LDA formalism.[38,39] The Thomas–Fermi screening length (kTF) of sX-LDA is determined by evaluating the dynamical average charge densities within our newly predicted structures. We took this feature to accomplish the predictions of the electronic structures of the newly determined structures. This is currently unavailable in VASP but we still rely on VASP predicted geometry structures due to its perfect balance between efficiency and accuracy. The phonon calculations are carried out by using a supercell method as implemented in the PHONOPY code.

3. Results and discussion

Figure 1 shows the plots of the volume of unit cell versus pressure and the CNT structures under different compressions. We find that not only the hexagonal and cubic diamond but also Z-carbon and P-carbon can be prepared by compressing CNTs. In Fig. 1(a), two hops in volume are observed in the pressure range of 0 to 400 GPa. They correspond to not only the changes of volume but also the changes of shape of the (18, 0) CNT. The saltation of unit cell volume and deformation of CNTs indicate the occurrence of phase transition, where there appear three phases named phases I, II, and III, respectively. Phase I exists in a pressure range of 0 to 4 GPa, in which the (18, 0) CNT retains its tubular structure. The pressure-induced structure transition takes place, where the circular cross section of CNT changes into an oval one. Phase II appears at a pressure of 5 GPa, in which the (18, 0) CNT collapses and transforms into AB stacking graphite. Phase III appears when pressure is increased up to 70 GPa, in which graphite transforms into cubic-diamond. In Fig. 1(b), two hops in volume are observed in the pressure range of 0 to 400 GPa. Similarly, there are three carbon phases named phases I, II, and III, respectively. At the pressure 50 GPa, the deformed nanotube (7, 0) is crushed and transforms into hexagonal diamond. Similar phase transition paths are observed in Figs. 1(c) and 1(d). The cold compressions of (4, 4) and (3, 3) CNTs result in Z-carbon and P-carbon respectively.

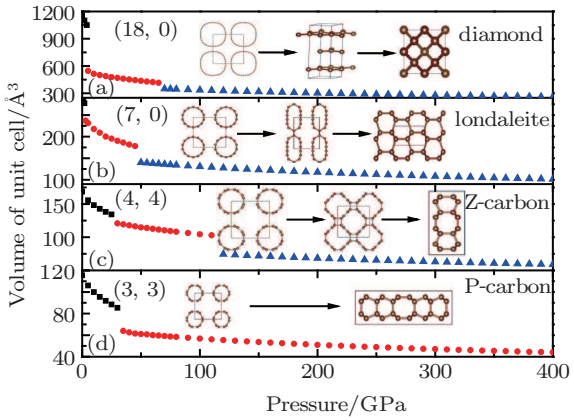


Fig. 1. (color online) Volumes of unit cell as a function of pressure.

Besides the known carbon phases mentioned above, numerous new carbon phases are produced by compressing CNT. In this work, we take two new phases as examples, which are obtained by compressing CNT (9, 0) and (4, 0) as shown in Fig. 2. These new phases with sp^3-hybridized bonds are marked by the parameter (m,n) of CNTs. The first new phase named (9, 0)-carbon is obtained by compressing the (9, 0) CNT when pressure is up to 45 GPa as shown in Fig. 2(a). This structrue has P_{mma} (D^5_{2h}) symmetry. The conventional unit cell for (9, 0)-carbon phase has 36 atoms with cell parameters of $a = 4.1538$ Å, $b = 11.2943$ Å, and $c = 4.3465$ Å at 0 GPa, yielding a cell volume of $V_0 = 203.91$ Å^3. The crystal structure of (9, 0)-carbon phase is similar to those of Z-carbon and P-carbon containing four-, six-, and eight-membered rings, in which four-membered and eight-membered rings join together buckled graphite sheets. In Fig. 2(b), the second new phase named (4, 0)-carbon is obtained by compressing (4, 0) CNTs when pressure is up to 255 GPa.

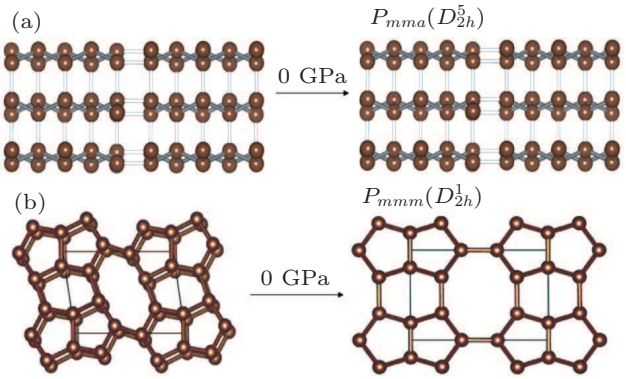


Fig. 2. (color online) Two new phases (constructed from the (9, 0), and (4, 0) CNTs under pressures above 45 GPa and 255 GPa, respectively) under different decompression conditions. The (9, 0) carbon has an antisymmetric structrue compared with the symmetric *bct*-C_4 structrue [Ref. [23]].

To evaluate the compressibility values of these new high pressure phases, the normalized volume as a function of pressure is displayed in Fig. 3. Meanwhile, anti-compressibility curves of the known phases, such as cubic diamond and cubic boron nitride (*c*-BN), are also provided in Fig. 3 for comparison. We find that the anti-compressibility values of these new carbon phases are larger than that of *c*-BN and smaller than that of cubic diamond.

The theoretical pressures as a function of the volume of diamond, (9, 0)-carbon, (4, 0)-carbon, and *c*-BN are fitted to the third-order Birch–Murnaghan equation of state to obtain the bulk modulus (B_0), as listed in Table 1. Strikingly, the bulk moduli of the two new phases are larger than that of *c*-BN (373 GPa) and smaller than that of diamond (453 GPa). An important prerequisite for a superhard carbon material is a large mass density in addition to the high degree of sp^3 hybridization. For example, the density of (9, 0)-carbon is 3.53 g/cm^3, which is much higher than that of graphite (2.22 g/cm^3) and closer to that of diamond (3.63 g/cm^3). All the above results indicate that these new high pressure phases are superhard material and some of them can be comparable to that of diamond.

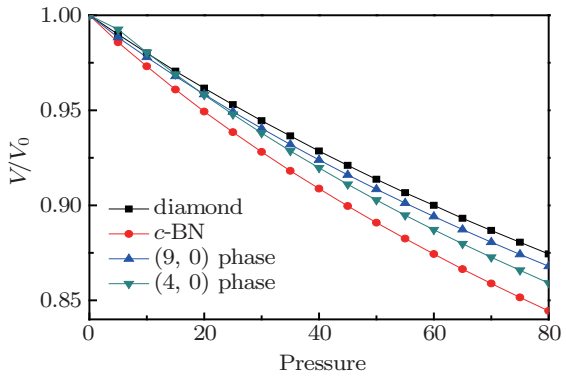


Fig. 3. (color online) Volume compressions as a function of pressure (unit: GPa) for different new carbon phases compared with *c*-BN and diamond.

Table 1. Space groups and values of lattice parameter (LP), density D (g/cm^3), band gap E_g (eV), and bulk modulus B_0 (GPa). Some experimental data are also listed for comparison.

Systems	Space group	LP/Å	D/g·cm^{-3}	E_g/eV	B_0/GPa
(9, 0) phase	P_{mma}	$a = 4.154$, $b = 11.294$ $c = 4.347$	3.53	4.81	441
(4, 0) phase	P_{mmm}	$a = 5.843$, $b = 3.869$ $c = 4.277$	3.30	5.39	401
Graphite	$P_{6_3/mmc}$	$a = b = 2.446$ $c = 6.527$	2.22		
c-BN	$F_{\bar{4}3m}$	$a = b = c = 3.625$ Å	3.45 3.49[40]	6.34 6.4[40]	373 391[40] 387[41]
Diamond	$F_{d\bar{3}m}$	$a = b = c = 3.533$ Å	3.64 3.63[41]	5.47 5.5[41]	453 446[41] 452[42]

In Fig. 4(a), the electronic band structure of (9, 0)-carbon is calculated. It is shown that the (9, 0)-carbon phase is a wide gap insulator with energy gap $E_g = 4.81$ eV (obtained by sX-LDA), which is lower than those of *c*-BN ($E_g = 6.34$ eV) and diamond ($E_g = 5.47$ eV). Furthermore, the band structure of the (4, 0)-carbon phase is calculated and the band gap is $E_g = 5.39$ eV as shown in Table 1. These results show that the (9, 0)-carbon and (4, 0)-carbon phases are transparent insulators. In order to confirm the dynamic stabilities of (9, 0)-carbon and (4, 0)-carbon phases, we calculate phonon spectra by using the supercell method. In this work, we take the (9, 0)-carbon phase for example as shown in Fig. 4(b). We find three phonon dispersion curves around the Γ point and no imaginary phonon frequencies in the whole brillouin zone. These results indicate that the (9, 0)-carbon phase is dynamically stable at zero pressure.

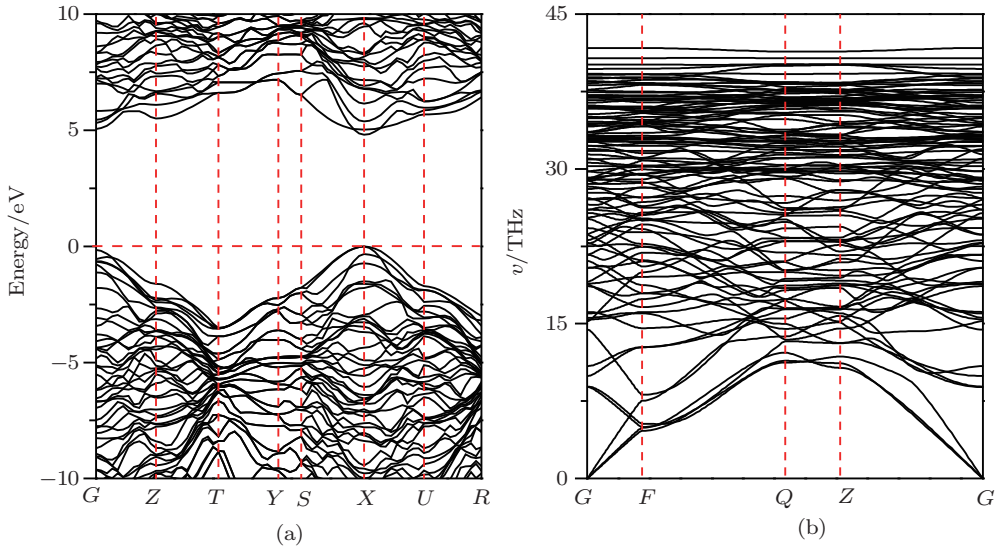


Fig. 4. (color online) Properties of the (9, 0) carbon phase at zero pressure: (a) electronic band structure; (b) phonon dispersion curves.

4. Conclusions

Some new carbon phases are obtained by compressing CNTs. Decompressing simulations demonstrate good stabilities of these new phases at ambient pressure with high bulk moduli compared with that of *c*-BN. The band structure calculations indicate that these phases are wide band gap insulators. From the results discussed above, we suggest that the cold-compression of the random placed CNTs produces the amorphous carbon first, and the amorphous structure of carbon further transforms into disordered sp^3-hybridized carbon under high pressure. The calculated results not only guide us in preparing the superhard carbon phases, but can also help us understand the structural phase transition of cold-compressed CNTs.

References

[1] Miller E D, Nesting D C and Badding J V 1997 *Chem. Mater.* **9** 18
[2] Hirsch A 2010 *Nat. Mater.* **9** 868
[3] Ehrenfreund P and Foing B H 2010 *Science* **329** 1159
[4] Bundy F P and Kasper J S 1967 *J. Chem. Phys.* **46** 3437
[5] Sumiya H and Irifune T 2007 *J. Mater. Res.* **22** 2345
[6] Irifune T, Kurio A, Sakamoto S, Inoue T and Sumiya H 2003 *Nature* **421** 599
[7] BAust R and Drickamer H G 1963 *Science* **140** 817
[8] Clarke R and Uher C 1984 *Adv. Phys.* **33** 469
[9] Bundy F P, Bassettb A W, Weathersb M S, Hemleyc R J, Maoc U H and Goncharovc A F 1996 *Carbon* **34** 141
[10] Wang Z W, ZhaoY S, Tait K, Liao X Z, Schiferl D, Zha C S, Downs R T, Qian J, Zhu Y T and Shen T D 2004 *Proc. Natl. Acad. Sci. USA* **101** 13699
[11] Tang J, Qin L C, Sasaki T, Yudasaka M, Matsushita A and Iijima S 2000 *Phys. Rev. Lett.* **85** 1887
[12] Khabashesku V N, Gu Z N, Brinson B, Zimmerman J L and Margrave J L 2002 *J. Phys. Chem. B* **106** 11155
[13] Popov M, Kyotani M, Nemanich R J and Koga Y 2002 *Phys. Rev. B* **65** 033408
[14] Popov M, Kyotani M and Koga Y 2003 *Diam. Relat. Mater.* **12** 833
[15] Bucknum M J and Castro E A 2006 *J. Chem. Theor. Comput.* **2** 775
[16] Kumar R S, Pravica M G, Cornelius A L, Nicol M F, Hu M Y and Chow P C 2007 *Diamond Relat. Mater.* **16** 1250
[17] Li Q, Ma Y M, Oganov A R, *et al*. 2009 *Phys. Rev. Lett.* **102** 175506
[18] Oganov A R and Glass C W 2006 *J. Chem. Phys.* **124** 244704
[19] Selli D, Baburin I A, Martonnak R and Leoni S 2011 *Phys. Rev. B* **84** 161411
[20] Amsler M, Flores-Livas J A, Lehtovaara L, Balima F, Ghasemi S A, Machon D, Pailhès S, Willand A, Caliste D, Botti S, Miguel A S, Goedecker S and Marques M A L 2012 *Phys. Rev. Lett.* **108** 065501
[21] Zhao Z S, Xu B, Zhou X F, Wang L M, Wen B, He J L, Liu Z Y, Wang H T and Tian Y J 2011 *Phys. Rev. Lett.* **107** 215502
[22] Wang J T, Chen C F and Kawazoe Y 2011 *Phys. Rev. Lett.* **106** 075501
[23] Umemoto K, Wentzcovitch R M, Saito S and Miyake T 2010 *Phys. Rev. Lett.* **104** 125504
[24] Niu H Y, Chen X Q, Wang S B, Li D Z, Mao W L and Li Y Y 2012 *Phys. Rev. Lett.* **108** 135501
[25] Elliott J A, Sandler J K W, Windle A H, Young R J and Shaffer M S P 2004 *Phys. Rev. Lett.* **92** 095501
[26] Pugno N M and Elliott J A 2012 *Physica E* **44** 944
[27] Gadagkar V, Maiti P K, Lansac Y, Jagota A and Sood A K 2006 *Phys. Rev. B* **73** 085402
[28] Yang X, Wu G and Dong J 2006 *Appl. Phys. Lett.* **89** 113101
[29] Cerqueira T F T, Botti S, San-Miguel A and Marques M A L 2014 *Carbon* **69** 355
[30] Sun D Y, Shu D J, Ji M, Liu F, Wang M and Gong X G 2004 *Phys. Rev. B* **70** 165417
[31] Capaz R B, Spataru C D, Tangney P, Cohen M L and Louie S G 2004 *Phys. Status Solidi B* **241** 3352
[32] Kresse G and Fürthmuller J 1996 *Phys. Rev. B* **54** 11169
[33] San X J, Liu Z M, Ma Y M, Cui T, Liu B B and Zou G T 2009 *Chin. Phys. B* **18** 1201
[34] San X J, He Z, Ma Y M, Cui T, Liu B B and Zou G T 2008 *Chin. Phys. B* **17** 2222
[35] Blochl P E 1994 *Phys. Rev. B* **50** 17953
[36] Monkhorst H J and Pack J D 1976 *Phys. Rev. B* **13** 5188
[37] Perdew J P, Burke K and Ernzerhof M 1996 *Phys. Rev. Lett.* **77** 3865
[38] Clark S J, Segall M D, Pickard C J, Hasnip P J, Probert M I J, Refson K and Payne M C 2005 *Z. Kristallogr* **220** 567
[39] Seidl A, Gorling A, Vogl P, Majewski J A and Levy M 1996 *Phys. Rev. B* **53** 3764
[40] Mohammad S N 2002 *Solid State Electron.* **46** 203
[41] Goncharov A F, Crowhurst J C, Dewhurst J K, Sharma S, Sanloup C, Gregoryanz E, *et al*. 2007 *Phys. Rev. B* **75** 224114
[42] Li J F and Zhang R Q 2013 *Carbon* **63** 562